ORIGINAL ARTICLE

Cancer Science WILEY

Cancer-associated adipocytes promote pancreatic cancer progression through SAA1 expression

Masanori Takehara[1] iD | Yasushi Sato[1] | Tetsuo Kimura[1,2] | Kazuyoshi Noda[1] | Hiroshi Miyamoto[1] | Yasuteru Fujino[1] | Jinsei Miyoshi[1] | Fumika Nakamura[1] | Hironori Wada[1] | Yoshimi Bando[3] | Tetsuya Ikemoto[4] | Mitsuo Shimada[4] | Naoki Muguruma[1] | Tetsuji Takayama[1] iD

[1]Department of Gastroenterology and Oncology, Institute of Biomedical Sciences, Tokushima University Graduate School, Tokushima City, Japan

[2]Clinic Green House, Kochi, Japan

[3]Division of Pathology, Tokushima University Hospital, Tokushima City, Japan

[4]Department of Surgery, Institute of Health Biosciences, Tokushima University Graduate School, The University of Tokushima, Tokushima City, Japan

Correspondence
Tetsuji Takayama, Department of Gastroenterology and Oncology, Institute of Biomedical Sciences, Tokushima University Graduate School, Tokushima, 770-8503, Japan.
Email: takayama@tokushima-u.ac.jp

Abstract

Although pancreatic cancer often invades peripancreatic adipose tissue, little information is known about cancer-adipocyte interaction. We first investigated the ability of adipocytes to de-differentiate to cancer-associated adipocytes (CAAs) by co-culturing with pancreatic cancer cells. We then examined the effects of CAA-conditioned medium (CAA-CM) on the malignant characteristics of cancer cells, the mechanism underlying those effects, and their clinical relevance in pancreatic cancer. When 3T3-L1 adipocytes were co-cultured with pancreatic cancer cells (PANC-1) using the Transwell system, adipocytes lost their lipid droplets and changed morphologically to fibroblast-like cells (CAA). Adipocyte-specific marker mRNA levels significantly decreased but those of fibroblast-specific markers appeared, characteristic findings of CAA, as revealed by real-time PCR. When PANC-1 cells were cultured with CAA-CM, significantly higher migration/invasion capability, chemoresistance, and epithelial-mesenchymal transition (EMT) properties were observed compared with control cells. To investigate the mechanism underlying these effects, we performed microarray analysis of PANC-1 cells cultured with CAA-CM and found a 78.5-fold higher expression of SAA1 compared with control cells. When the *SAA1* gene in PANC-1 cells was knocked down with *SAA1* siRNA, migration/invasion capability, chemoresistance, and EMT properties were significantly attenuated compared with control cells. Immunohistochemical analysis on human pancreatic cancer tissues revealed positive SAA1 expression in 46/61 (75.4%). Overall survival in the SAA1-positive group was significantly shorter than in the SAA1-negative group (*P* = .013). In conclusion, we demonstrated that pancreatic cancer cells induced de-differentiation in adipocytes toward CAA, and that CAA promoted malignant characteristics of

pancreatic cancer via SAA1 expression, suggesting that SAA1 is a novel therapeutic target in pancreatic cancer.

KEYWORDS

cancer microenvironment, cancer-associated adipocytes, metastasis, pancreatic cancer, SAA1

1 | INTRODUCTION

Pancreatic ductal adenocarcinoma (PDAC) is the third-leading cause of cancer-related deaths worldwide.[1] Although surgical resection is the only curative treatment for PDAC, most PDAC cases are inoperable because of aggressive local invasion and early distant metastasis.[2] Moreover, current chemotherapeutic agents have low efficacy; median OS in patients with inoperable PDAC is only 14 mo.[3]

One of the pathological characteristics of PDAC is a profuse desmoplastic tumor stromal component, which represent up to 90% of the tumor volume.[4-6] Tumor stroma is known to have a heterogeneous microenvironment,[7,8] consisting of cancer-associated fibroblasts (CAFs),[9,10] pancreatic stellate cells,[11,12] immune cells,[13] endothelial cells, and extracellular matrices,[14] and has been shown to promote cell growth and invasion and to contribute to reduced delivery of chemotherapeutic agents. Therefore, tumor stroma is thought to be one of the main contributors to chemotherapy resistance, and therapies targeting stroma are expected to improve overall treatment efficacy.[14,15] While several agents targeting stromal components have been developed,[15,16] no substantially effective anti-stromal therapy is available for clinical use. Thus, further studies are required to understand the complex interaction between pancreatic tumors and stromal cells, and such knowledge could ultimately lead to therapeutic benefits for PDAC patients.

To date, some epidemiological investigations have revealed that obesity increases the risk of pancreatic cancer development.[1,17-20] Moreover, peripancreatic fat invasion is an independent predictor of a poor prognosis following surgery for PDAC.[21] In a mouse model of PDAC, EL-KrasG12D/PEDF-deficient mice developed invasive PDAC associated with increased peripancreatic fat.[22] Similarly, mice with a conditional KrasG12D mutation fed a high-fat diet showed increases in the numbers of precancerous lesions and invasive cancer.[23,24] These findings support the notion that adipose tissue has a tumor-promoting role in the PDAC microenvironment. However, the underlying mechanisms of cancer progression via the cancer-adipocyte interaction are still poorly understood.

The pancreas is a retroperitoneal organ surrounded by adipose tissue and, therefore, PDAC easily invades into the peripancreatic adipose tissue; this supports the idea that adipocytes could be an important stromal component for tumor progression in patients with PDAC. In breast cancer, invasive cancer cells dramatically affect surrounding adipocytes, causing profound phenotypic changes both in vitro and in vivo. These peritumoral adipocytes tend to be smaller in size than those distant from the cancer.[25] Dirat and associates referred to these modified adipocytes as CAA and showed that CAA

promotes invasion and metastasis of breast cancer cells.[26] However, little information is known about the biological and molecular mechanisms involved in the interaction between pancreatic cancer cells and CAA that could affect pancreatic cancer progression.

Therefore, in this study, we first investigated if mature adipocytes are morphologically and biologically altered to become CAA by co-culturing them with pancreatic cancer cells, and then examining the effects of CAA-conditioned media (CAA-CM) on cell proliferation, migration/invasion capability, drug resistance, and induction of EMT in pancreatic cancer cells. Moreover, we performed microarray analysis to detect significant changes of gene expression in CAA-CM-treated pancreatic cancer cells. As we ultimately identified serum amyloid A1 (SAA1) as a specifically upregulated gene in pancreatic cancer cells, we evaluated the clinical relevance of SAA1 expression in patients with PDAC in association with their clinicopathological factors.

2 | MATERIALS AND METHODS

2.1 | Cell culture and adipocyte differentiation

Three human pancreatic cancer cell lines, PK1, PK-45H, and PK-8, were obtained from the RIKEN Cell Bank (Saitama, Japan). Two human pancreatic cancer cell lines, MIA PaCa-2, PANC-1, and 3T3-L1 cells—the latter being a stable and replicable adipocyte-differentiating cell line—were obtained from the American Type Culture Collection (ATCC). Adipocyte differentiation of 3T3-L1 was induced as previously described.[27] Differentiated 3T3-L1 adipocyte stromal cells (3T3-L1 adipocyte) were stained with Oil Red O and the dye retained in the cells was eluted into isopropanol. Absorbance at 496 nm was then determined to quantify the lipid contents.

2.2 | Induction of cancer-associated adipocytes

To induce CAA, 3T3-adipocytes were co-cultured indirectly with PANC-1 cells using a Transwell cell culture insert (ThinCert™ 657641; Greiner Bio-One) in DMEM supplemented with 10% FBS. PANC-1 cells were seeded onto the upper chamber (1×10^5 cells/well) and 3T3-adipocytes were seeded onto the lower chamber (4×10^4 cells/well), followed by co-cultivation for 6 d. A half volume of the co-culture medium was replaced every 3 d and 3T3-L1 adipocytes were cultivated alone as controls. To generate CM from CAA (CAA-CM), CAA was cultured alone with FBS-free DMEM for 24 h after being

washed twice with PBS. The medium was then collected and filtered using a 0.25-μm-pore filter and stored 4°C until use within 1 mo.

2.3 | Proliferation assay

Cell proliferation was analyzed using a cell counting kit (CCK-8; Dojindo) according to the manufacturer's instructions.

2.4 | Western blot analysis

Western blot analysis was performed, as described in Appendix S1. The primary antibodies used are listed in Table S1.

2.5 | Drug sensitivity

Drug sensitivity of the cells to 5-fluorouracil (5-FU) was determined using a CCK-8 assay, as previously described.[28] IC_{50} values were determined by non-linear regression analysis using GraphPad Prism software (GraphPad Prism v.8.0).

2.6 | Microarray analysis

The mRNAs extracted from PANC-1 cells incubated with CAA-CM or DMEM were labeled with cyanine-3 (cRNA) using a Low Input Quick Amp Labeling Kit (Agilent Technologies). The cRNAs were applied to the slides and analyzed on a Agilent SurePrint G3 8 × 60K array. Quantile normalization and subsequent data processing were performed using the GeneSpring GX v.11.5.1 software package (Agilent Technologies).

2.7 | Quantitative real-time PCR

Quantitative real-time PCR was performed as described previously.[29] The pre-designed TaqMan Gene Expression Assays (Applied Biosystems) used are described in Table S2.

2.8 | Immunofluorescence

Immunofluorescence staining for adipocytes and PANC-1 cells was performed, as described in Appendix S1. The stained cells were observed using a fluorescence microscope (BZ-X 700; Keyence, Osaka, Japan).

2.9 | Patients

We retrospectively enrolled 61 patients with PDAC surgically resected between February 2010 and October 2017 at Tokushima University Hospital. This study was conducted in accordance with the Declaration

of Helsinki and approved by the Ethical Review Board of Tokushima University Hospital. RFS was defined as the time from surgery to first evidence of recurrent disease or death from any cause. OS was defined as the interval between the date of surgery and cancer-related death. Patients known to be alive without recurrent disease or lost to follow-up at the time of analysis were censored at the time of their last follow-up.

2.10 | Immunohistochemistry

Immunohistochemical staining for SAA1 in paraffin-embedded tissue sections was performed, as described in Appendix S1. A mouse anti-human SAA1 monoclonal antibody (Sigma-Aldrich) was used as the primary antibody. Staining intensity and positivity for SAA1 expression in cancer cells were assessed using the Histo-score (H-score), which was established by Yang and colleagues for SAA1 staining in breast cancer tissues.[30] Briefly, staining at the invasive front was scored by intensity (0 = none, 1+ = weak, 2+ = moderate, 3+ = strong), as described in Figure S1, and the percentage of tumor cells stained for each intensity. The H-score was calculated using the following formula: (3 × percentage of strong staining) + (2 × percentage of moderate staining) + (1 × percentage of weak staining). Scoring was performed in at least 3 regions (540 μm × 720 μm) in each case and averaged. Based on a previous study on immunohistochemistry for SAA1 in breast cancer,[30] the cut-off value was set at 100 and SAA1 expression was classified into 2 groups; an H-score from 0 to 99 represented negative expression and an H-score of 100-300 represented positive expression.

2.11 | Statistical analysis

Student *t* test was used to compare paired continuous variables. Fisher exact test was used to compare categorical data. Univariate survival analysis was performed using the Kaplan-Meier method. Survival curves were compared by log-rank test. Univariate and multivariate analyses were performed using the Cox proportional hazards model.

Wound healing assay, cell invasion assay, and small interfering RNA transfection procedures are described in Appendix S1.

3 | RESULTS

3.1 | 3T3-L1 adipocytes exhibited extensive phenotypical changes following co-culture with pancreatic cancer cells

To investigate how the characteristics of 3T3-L1 adipocytes could be modified following interaction with pancreatic cancer cells in vitro, we employed an indirect co-culture system in which PANC-1 cells were seeded in the top chamber and 3T3-L1 adipocytes in the bottom chamber of a Transwell. We first examined cell morphology using Oil Red O staining under a microscope. Figure 1A shows representative images of

3T3-L1 adipocytes with or without co-culture with PANC-1 cells. After 8 d of co-culture, the adipocytes became elongated in shape, similar to a fibroblast morphology, and lost a considerable amount of lipid droplets, which were not observed in adipocytes cultured with maintenance medium alone. Quantitative analysis revealed that the lipid content in adipocytes incubated with PANC-1 cells was significantly lower than that in control 3T3-L1 adipocytes (Figure 1B; $P < .001$). In the analysis of mature adipocyte-specific gene expression, the mRNA levels for Pparg and Fabp4 in 3T3-L1 adipocytes co-cultured with PANC-1 cells were significantly lower than those in control 3T3-L1 adipocyte cells (Figure 1C; $P < .05$). Moreover, the mRNA level of Adipoq in those adipocytes was marginally lower than that in control cells (Figure 1C; $P = .065$).

Conversely, the mRNA levels of S100a4 and α-smooth muscle actin (α-SMA) in 3T3-L1 adipocytes co-cultured with PANC-1 cells were significantly higher than that in control cells (Figure 1C; $P < .01$). The adipocytes stained faintly for α-SMA at d 3, moderately at d 5, and then strongly at d 8. A similar staining pattern for S100a4 was observed in 3T3-L1 adipocytes co-cultured with PANC-1 cells (Figure 1D). Thus, adipocytes co-cultivated with PANC-1 cells exhibited a loss of lipid content, a decrease in adipose markers, and emergence of fibroblast markers, strongly suggesting a process of de-differentiation of adipocytes toward fibroblast-like cells. These phenotypic changes were consistent with previously described characteristics of breast CAA following stimulation by cancer cells.[26] The results obtained in experiments with PK-1 cells were similar
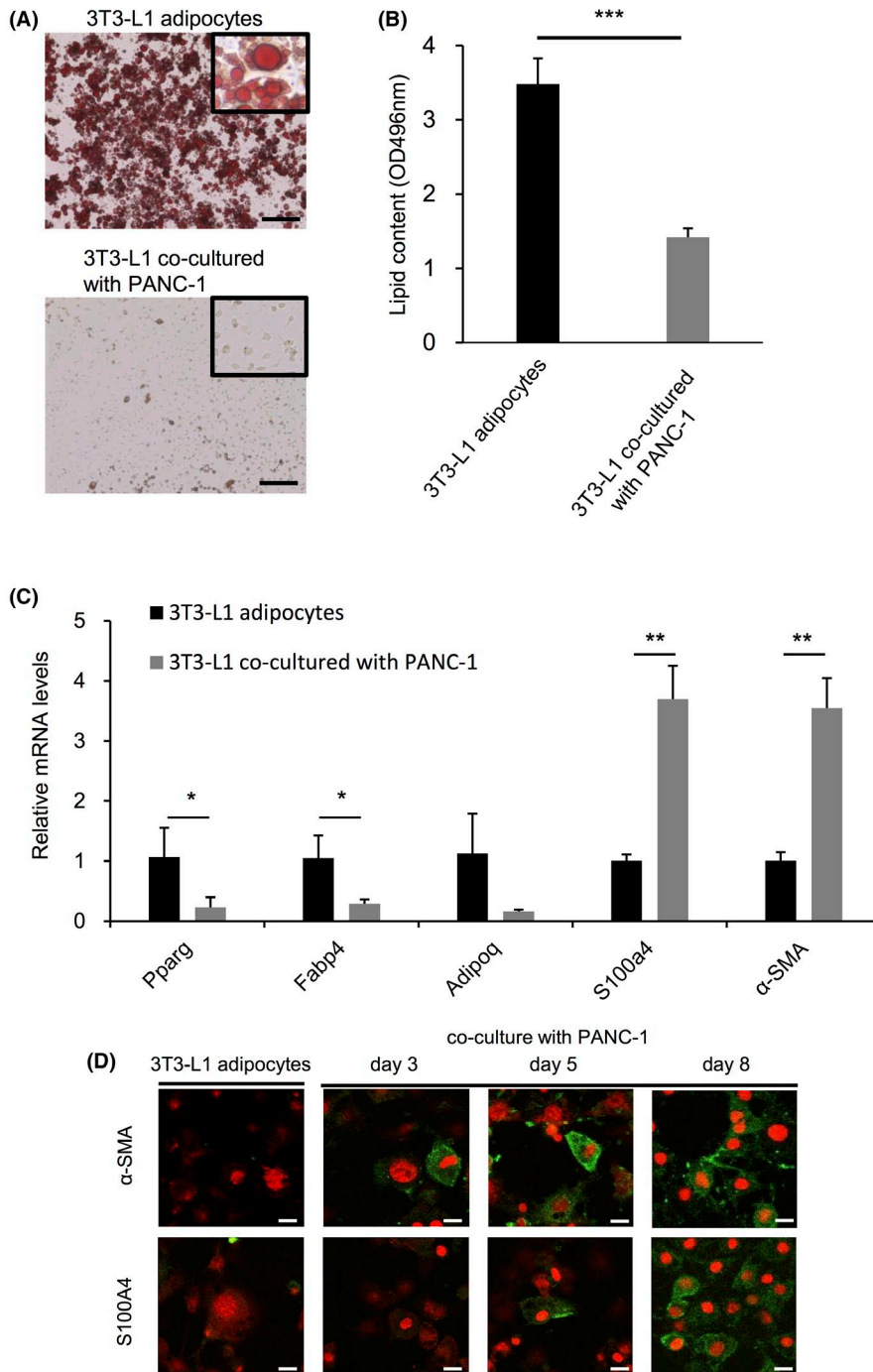

FIGURE 1 Change of 3T3-L1 adipocytes to cancer-associated adipocytes (CAAs) following co-culture with PANC-1 cells. A, Mature 3T3-L1 adipocytes (upper panel) and 3T3-L1 adipocytes co-cultured with PANC-1 cells (lower panel) were stained with Oil Red O. A magnified image is shown in each inset, scale bars, 100 μm. B, The amount of lipid was determined by extracting the Oil Red O with isopropanol and measuring the absorbance at 496 nm; n = 3. C, Levels of mRNA for adipogenesis markers (Pparg, Fabp4, Adipoq) and fibroblastic markers (S100a4, α-SMA) in mature 3T3-L1 adipocytes and 3T3-L1 adipocytes co-cultured with PANC-1 cells were measured by quantitative PCR; n = 3. D, Immunofluorescence for α-SMA and S100A4 was performed in mature 3T3-L1 adipocytes co-cultured with PANC-1 cells. 3T3-L1 adipocytes grown on coverslips were co-cultured with PANC-1 cells for 3, 5, or 8 d; fixed with 4% paraformaldehyde (PFA); permeabilized with 0.1% Triton X-100; and incubated with a rabbit anti-mouse α-SMA monoclonal antibody or a rabbit anti-mouse S100A4 polyclonal antibody following incubation with secondary antibody conjugated with FITC. The cells were observed under a fluorescence microscope. 3T3-L1 mature adipocytes served as a control. Scale bars, 10 μm. *$P < .05$, **$P < .01$, ***$P < .001$

FIGURE 2 Cell proliferation, migration/invasion capability, resistance to 5-fluorouracil (5-FU), and epithelial-mesenchymal transition in PANC-1 cells cultured with conditioned media from CAA. A, Proliferation of PANC-1 cells cultured with CAA-CM or control medium was analyzed by WST-8 assay; n = 3. B, The migrated area in PANC-1 cells cultured with CAA-CM or control medium was assessed using a wound healing assay, and quantified with TScratch software; n = 3. Scale bars, 200 μm. C, Invasion capability of PANC-1 cells cultured with CAA-CM or control medium was assessed by Transwell invasion assay. The invading cells were stained using cell stain solution and quantified by measuring absorbance; n = 3. Scale bar, 200 μm. D, PANC-1 cells seeded in 96-well plates were cultured with CAA-CM or control medium for 72 h. The cells were then treated with different concentrations of 5-FU (0.1-1000 μmol/L) for 72 h, and viable cells were quantified by WST assay. IC_{50} values were determined by non-linear regression analysis; n = 3. E, Western blot analyses were performed for E-cadherin, N-cadherin, Snail, and Slug in PANC-1 cells cultured with CAA-CM or control medium. F, Immunofluorescence was measured for E-cadherin and N-cadherin in PANC-1 cells cultured with CAA-CM or control medium, as described in Materials and Methods. Scale bars, 10 μm * P < .05
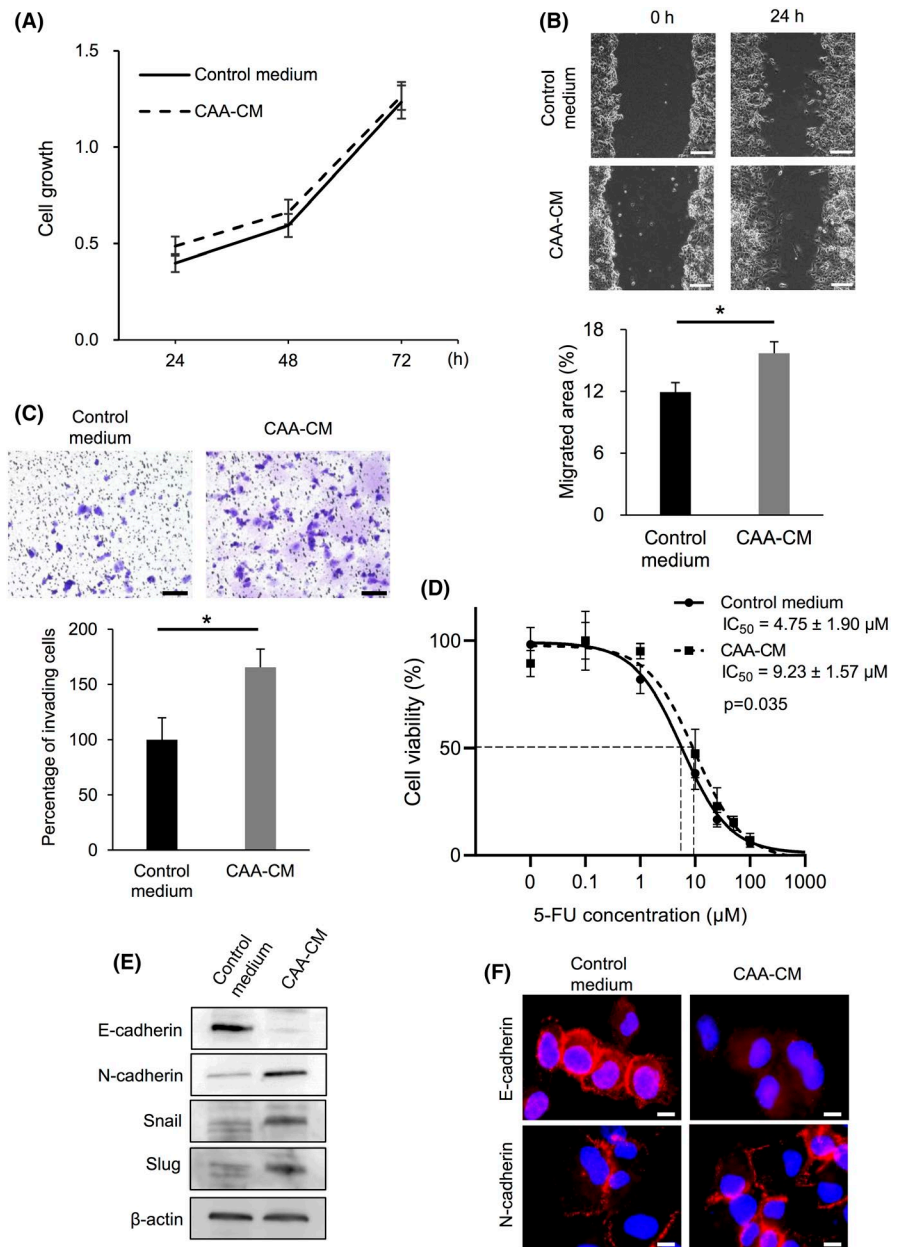
to those with PANC-1 cells (Figure S2). In addition, we found that all 5 human pancreatic cancer cell lines changed adipocytes morphologically into CAAs by co-culture in a Transwell (Figure S3A). Those CAAs showed a fibroblast-like morphology and lost considerable amounts of lipid droplets (Figure S3B). These findings suggest that the cancer-adipocyte interaction is a general event in pancreatic cancer tissues.

3.2 | Effects of CAA-derived conditioned medium on cell proliferation, migration, invasiveness, and chemotherapy sensitivity of PANC-1 and PK-1 cells

To examine the effect of CAA-CM on proliferation of pancreatic cancer cells, we first cultured PANC-1 or PK-1 cells with CAA-CM and then assessed cell proliferation by WST-8 assay. No significant differences in proliferation of PANC-1 cells were observed between the CAA-CM and control medium groups (Figure 2A). We then performed a scratch wound assay to test cell migration activity. Representative images of wound healing in PANC-1 cells co-cultured with CAA-CM and control medium are shown in Figure 2B. Quantitative analysis of images showed that the migration rate in PANC-1 cells with CAA-CM (15.70 ± 1.13%) was significantly higher than with control medium (11.93 ± 0.91%, P = .011). An invasion assay was also performed and the representative images are shown in Figure 2C. Quantitative analysis revealed that the number of invading cells after co-culture with CAA-CM was significantly higher than in control cells (Figure 2C; P = .012). We next examined the effect of CAA-CM on the sensitivity of PANC-1 cells to 5-FU. The IC_{50} for PANC-1 cells cultured with CAA-CM (9.23 ± 1.57 μmol/L) was significantly higher than for control cells (4.75 ± 1.90 μmol/L,

(A)

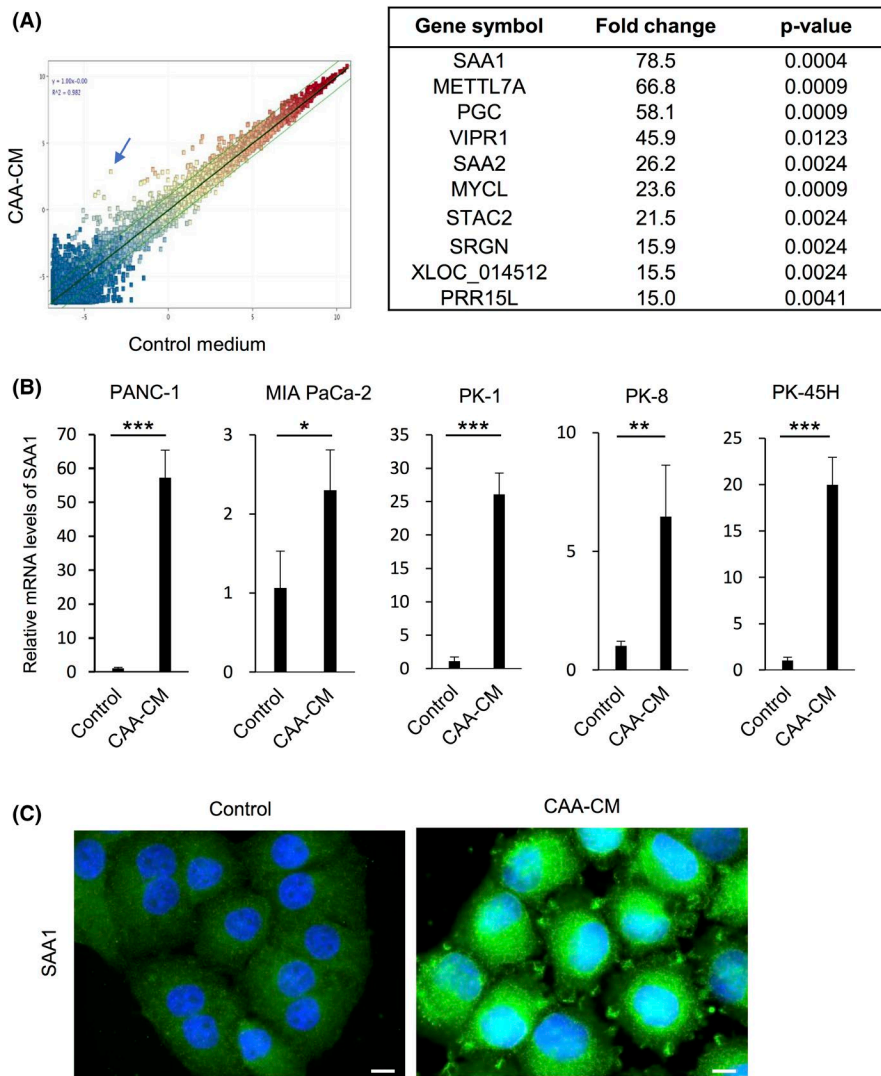| Gene symbol	Fold change	p-value
SAA1	78.5	0.0004
METTL7A	66.8	0.0009
PGC	58.1	0.0009
VIPR1	45.9	0.0123
SAA2	26.2	0.0024
MYCL	23.6	0.0009
STAC2	21.5	0.0024
SRGN	15.9	0.0024
XLOC_014512	15.5	0.0024
PRR15L	15.0	0.0041

(B)

(C)

FIGURE 3 SAA1 upregulation in pancreatic cancer cells incubated with CAA-CM. A, A representative scatter plot of microarray data from PANC-1 cells incubated with CAA-CM and control medium is shown. The top 10 upregulated genes obtained from triplicate experiments are shown in the right panel; n = 3. The arrow indicates SAA1 in the left panel. B, Five pancreatic cancer cell lines were incubated with CAA-CM or control medium for 3 d and SAA1 mRNA levels were quantified by real-time PCR; n = 4. C, Immunofluorescence was performed for SAA1 in PANC-1 cells incubated with CAA-CM or control medium. The cells were fixed with 4% PFA, permeabilized with 0.1% Triton X-100, and incubated with mouse anti-human SAA1 antibody and secondary antibody conjugated with FITC. DAPI was used for nuclear staining. The cells were observed under a fluorescence microscope. Scale bars, 10 μm. *P < .05, **P < .01, ***P < .0001

P = .035), indicating that CAA-CM significantly reduced the sensitivity of PANC-1 cells to 5-FU (Figure 2D). Results obtained in experiments with PK-1 cells were similar to those with PANC-1 cells (Figure S4).

## 3.3 | CAA-CM modulated EMT properties in PANC-1 cells

Because EMT is known to be closely related to cancer invasion and migration,[31] we examined expression of EMT-associated proteins by western blot analysis. Expression of E-cadherin in PANC-1 cells cultured with CAA-CM was significantly lower than in control cells. In contrast, expression of N-cadherin, Snail, and Slug in PANC-1 cells cultured with CAA-CM was noticeably higher than in control cells (Figure 2E). Moreover, immunofluorescence revealed that E-cadherin expression in the membrane of PANC-1 cells cultured with CAA-CM was markedly decreased compared with that of control cells. Conversely, N-cadherin expression in the membrane of PANC-1 cells cultured with CAA-CM was enhanced compared with

that of control cells (Figure 2F). These results strongly suggest that CAA-CM promoted EMT in PANC-1 cells.

3.4 | CAA-CM upregulated SAA1 expression in pancreatic cancer cell lines

To clarify the mechanisms by which CAA-derived factors modulate cell migration, invasion, and EMT, we performed a microarray analysis to detect changes in the mRNA expression profile of PANC-1 cells after CAA-CM treatment. A representative scatter plot is shown in Figure 3A. Analysis of average mRNA expression from triplicate microarray data revealed that 10 genes were upregulated (>15-fold) in PANC-1 cells treated with CAA-CM compared with control medium alone. Of these, SAA1 was chosen as the most relevant gene because its expression level was the highest (at 78.5-fold) and was associated with the lowest P-value (P = .0004). Upregulation of SAA1 mRNA was also confirmed in various pancreatic cancer cells lines, including MIA PaCa-2, PK-45H, PK-1, and PK-8 cells, after treatment with CAA-CM

FIGURE 4 Cell proliferation, migration/invasion capability, drug resistance to 5-FU, and EMT in PANC-1 cells transfected with SAA1 siRNA following incubation with CAA-CM. A, Proliferation of PANC-1 cells transfected with SAA1 siRNA or scramble siRNA were analyzed by WST-8 assay; n = 6. B, Migration of PANC-1 cells transfected with SAA1 siRNA or scramble siRNA was assessed by wound healing assay. Migrated areas were quantified using TScratch software; n = 6. Scale bars, 200 μm. C, Invasion capability of PANC-1 cells transfected with SAA1 siRNA or scramble siRNA were assessed by Transwell invasion assay. Invading cells were quantified by measuring absorbance; n = 6. Scale bars, 200 μm. D, PANC-1 cells transfected with SAA1 siRNA or scramble siRNA were treated with different concentrations of 5-FU for 72 h. Viable cells were quantified by WST assay; n = 6. E, Western blot analyses were performed for E-cadherin, N-cadherin, Snail, and Slug in PANC-1 cells transfected with SAA1 siRNA or scramble siRNA. *$P < .05$, **$P < .01$
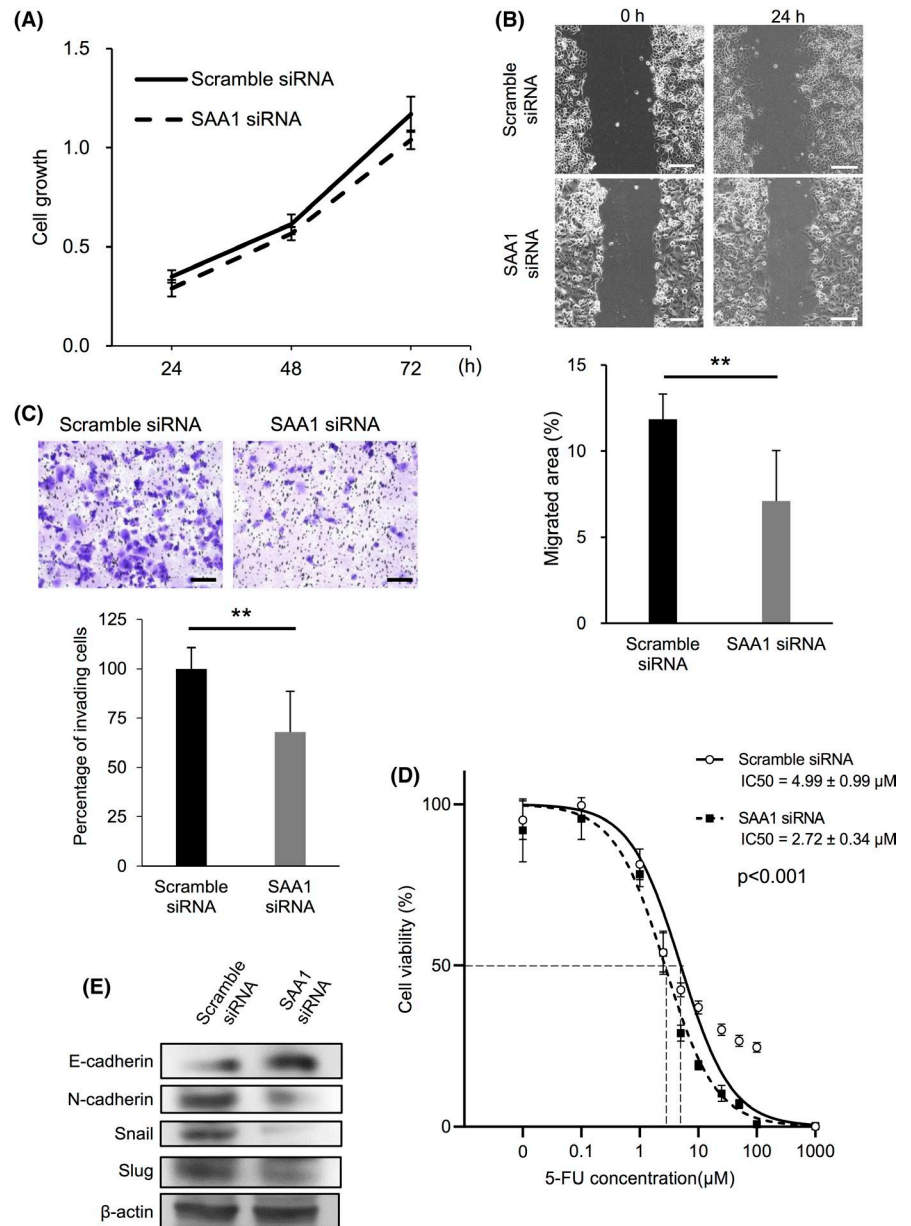
(Figure 3B). Immunofluorescent staining revealed that SAA1 was overexpressed mainly in the cytosol of PANC-1 cells after treatment with CAA-CM (Figure 3C).

3.5 | Knockdown of *SAA1* modulated cell invasion/migration, chemotherapy resistance, and EMT properties of PANC-1 cells

To further investigate the role of SAA1 induced in PANC-1 cells, we examined whether *SAA1* gene knockdown could affect the proliferation, migration/invasion, chemotherapy sensitivity, and EMT properties of PANC-1 cells cultured with CAA-CM. Successful knockdown of *SAA1* siRNA was confirmed by the finding that *SAA1* mRNA levels in PANC-1 cells transfected with *SAA1* siRNA were decreased by approximately 90%-95% at 24-120 h compared

with control scramble siRNA (Figure S5). There was no significant difference in cell growth between *SAA1* siRNA-transfected cells and control cells transfected with scramble siRNA (Figure 4A). However, in the wound healing assay, the migration rate of *SAA1* siRNA-transfected cells (7.10 ± 2.92%) was significantly lower than that of the control cells (11.85 ± 1.46%, $P = .005$; Figure 4B). Similarly, quantitative analysis revealed that the number of invading cells in *SAA1* siRNA-transfected PANC-1 cells was significantly lower than in control cells ($P = .007$; Figure 4C). When the sensitivity of PANC-1 cells to 5-FU was examined by cell viability assay, the IC_{50} value in *SAA1* siRNA-transfected PANC-1 cells (2.72 ± 0.34 μmol/L) was significantly lower than in the control cells (4.99 ± 0.99 μmol/L, $P < .001$), indicating that SAA1 indeed plays a pivotal role in drug resistance to 5-FU (Figure 4D). The results obtained in experiments with PK-1 cells were similar to those with PANC-1 cells (Figure S6).

We next examined the expression of EMT-associated proteins by western blotting (Figure 4E). Expression of E-cadherin in siRNA *SAA1*-transfected cells was significantly higher than in control cells, while the expression of N-cadherin, Snail, and Slug was significantly lower than in control cells. These data strongly suggest that SAA1 overexpression induced by CAA-CM acts as a critical modulator of invasion, migration, chemoresistance, and induction of EMT in PANC-1 cells.

3.6 | SAA1 expression was associated with a poor prognosis in patients with PDAC

To investigate the clinical significance of SAA1 expression, we next examined the possible correlation between the prognosis of PDAC patients and SAA1 expression in resected cancer tissues as determined by immunohistochemical staining. Patient characteristics are shown in Table 1. Of the 61 patients, 34 were men. The median age was 68 y (range, 42-89 y). The pathological T stages were pT1 + T2 and pT3 + T4 in 50 and 11 patients, respectively. In total, 20 patients had lymph node metastasis. Histological grade 2 (G2) was the most frequent (28/64), followed by G1 (24/64), G3 (6/64) and other types (3/64). CA19-9 values greater than 300 were detected in 25 patients. Forty-seven patients received perioperative chemotherapy. Representative staining patterns for SAA1 are shown in Figure 5A, B. Strong staining for SAA1 was seen in the cytoplasm of tumor cells from case 1 (Figure 5A), whereas almost no staining was observed in tumor cells from case 2 (Figure 5B). SAA1 was strongly stained in normal liver tissue (positive control) (Figure 5C). SAA1 staining was positive in 46 of 61 cancer tissues (75.4%). Moreover, the cancer tissue surrounded by adipose tissue showed stronger staining for SAA1 compared with those without surrounding adipose tissue. Table 2 shows the clinicopathological characteristics of patients with SAA1-positive and SAA1-negative tumors. There were no significant differences in age, gender, T-stage, lymph node metastasis, histological grade, CA19-9 levels, or perioperative chemotherapy status between the SAA1-positive and SAA1-negative groups. The median RFS in the SAA1-positive group (7.7 mo, 95% confidence interval [CI] 4.7-12.2) tended to be shorter than that in the SAA1-negative group (21.7 mo, 95% CI 6.0-not available [NA]) (P = .083). The median OS in the SAA1-positive group was 23.4 mo (95% CI 12.2-NA), whereas it was not reached in the SAA1-negative group (95% CI 35.7-NA) There was a significant difference between the 2 groups (P = .013, Figure 5E). Univariate analysis of clinicopathological factors for OS revealed that depth (T-stage) of primary tumor (P = .029), lymph node stage (P = .020), CA19-9 value (P = .024), and SAA1 positivity (P = .023) were significant factors. Multivariate analysis of these factors revealed that SAA1 expression (P = .018) and CA19-9 (300≤, P = .045) could be independent prognostic markers for OS (Table 3).

4 | DISCUSSION

In this study, we found that adipocytes co-cultured with pancreatic cancer cells changed morphologically into fibroblast-like cells and

TABLE 1 Patients' characteristics

Characteristic	n = 61
Age (y, median)	42-89 (68)
Gender	
Male	34 (55.7%)
Female	27 (44.3%)
Primary tumor[a]	
T1 + 2	50 (82.0%)
T3 + 4	11 (18.0%)
Lymph node metastasis	
Negative	41 (67.2%)
Positive	20 (32.8%)
Histological grade	
G1 (wel[b])	24 (39.3%)
G2 (mod[c])	28 (45.9%)
G3 (por[d])	6 (9.8%)
Other type (muc[e])	3 (4.9%)
CA19-9 (U/mL)	
<300	36 (59.0%)
≥300	25 (41.0%)
Perioperative chemotherapy[f]	
–	14 (23.0%)
+	47 (77.0%)

[a]T-stage was evaluated according to the criteria of International Union for Cancer Control (UICC) 8th edition.
[b]Well differentiated adenocarcinoma.
[c]Moderately differentiated adenocarcinoma.
[d]Poorly differentiated adenocarcinoma.
[e]Mucinous carcinoma.
[f]Adjuvant chemotherapy was performed for 41 cases and neoadjuvant chemotherapy was performed for 8 cases; 2 cases received both therapies.

expressed fibroblast-specific gene markers, strongly suggesting de-differentiation/reprograming of adipocytes toward CAA. We also demonstrated that CAA-CM enhanced migration/invasion capability and chemoresistance, and promoted EMT in pancreatic cancer cells, by upregulating SAA1 in those cells. Moreover, our data for surgically resected PDAC tissues revealed a significant correlation between SAA1 expression and survival times, suggesting that SAA1 is an independent prognostic marker for a poor prognosis in patients with PDAC.

We first showed that co-culture of adipocytes and pancreatic cancer cells in a Transwell system caused characteristic phenotypes in adipocytes: ie, morphological change of adipocytes into fibroblast-like cells, which showed much lower lipid levels; loss of adipocyte-specific markers such as Adipoq, Pparg and Fabp4; and expression of fibroblast-specific S100a4 and α-SMA. Moreover, we observed fibroblast-like cell clusters showing a smaller and more elongated shape with positivity of α-SMA and S100A4 at the invasion site of pancreatic cancer cells into adipose stroma from human surgically resected

FIGURE 5 SAA1 expression and recurrence free survival and overall survival in pancreatic cancer patients. A-C, Representative images of immunohistochemistry for SAA1 in pancreatic cancer tissues are shown. A, SAA1 positive; scale bars, 50 μm. B, SAA1 negative. C, Hepatocytes as a positive control. D, Kaplan-Meier analysis was performed to evaluate the correlation between RFS and SAA1 expression in pancreatic cancer. E, Kaplan-Meier analysis was performed to evaluate the correlation between overall survival and SAA1 expression in pancreatic cancer
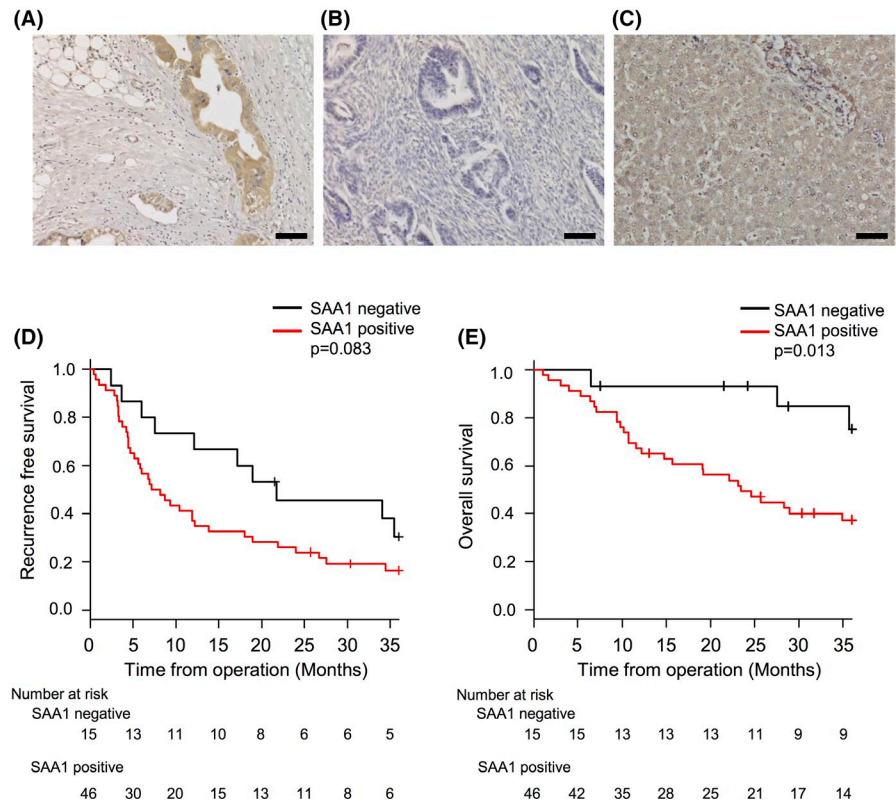

TABLE 2 Patient information and clinicopathologic parameter correlations with SAA1 expression

	SAA1-positive n = 46	SAA1-negative n = 15	P-value
Age (y, median)	42-89 (66)	57-86 (70)	.063
Gender			
Male	27	7	.551
Female	19	8	
Primary tumor			
T1 + 2	37	13	.716
T3 + 4	9	2	
Lymph node metastasis			
Negative	29	12	.344
Positive	17	3	
Histological grade			
G1	18	6	.959
G2	20	8	
G3	5	1	
Other type (muc)	3	0	
CA19-9 (U/mL)			
<300	27	9	1.00
≥300	19	6	
Perioperative chemotherapy			
−	11	3	1.00
+	35	12	

PDAC tissues (Figure S7). These in vitro and in vivo phenotypic changes of adipocytes following interaction with pancreatic cancer cells are consistent with the CAA characteristics first described in breast cancer[25] and provide additional evidence for findings reported recently of adipocytes and pancreatic cancer cell line interactions that demonstrated the appearance of fibroblast-like cells after co-culture of 3T3-L1 adipocytes and MIA PaCa2 in vitro.[32] To date, only a few studies have investigated the characteristics of CAA and CAF,[25,33] and it remains unclear and controversial how CAA differs from CAF.

We also demonstrated that CAA-CM affected cancer cell migration/invasion capability and acquisition of drug resistance to 5-FU and EMT. Notably, CAA-CM induced Snail and Slug expression, resulting in the EMT properties. It is well known that the pancreatic cancer microenvironment contains abundant stromal cells including CAF,[7] tumor-associated macrophage (TAM),[34] and endothelial cells, which often lead to a desmoplastic reaction. It is plausible that CAA enhances such malignant characteristics of the desmoplastic reaction together with CAF and TAM surrounding the cancer cells. Moreover, it has recently been reported that conditioned medium from omental fat tissues obtained from patients with pancreatic cancers and ovarian cancers promoted cell growth, migration/invasion capability, and drug resistance.[35,36] This indicates that not only CAA but also mature adipocytes can promote malignant potential in pancreatic cancers. Although we did not compare the effects of CM from CAA and mature adipocytes, the differences and underlying mechanisms should be clarified in the future.

Employing an unbiased approach with comprehensive microarray analysis, we identified SAA1 in PANC-1 cells whose expression

Variables	Univariate analysis		Multivariate analysis	
	HR (95% CI)	P-value	HR (95% CI)	P-value
Age (y)				
<70	1	.812		
≥70	1.09 (0.55-2.14)			
Gender				
Male	1	.505		
Female	1.259 (0.64-2.48)			
Primary tumor				
T1 + 2	1	.029	1	.162
T3 + 4	2.36 (1.09-5.11)		1.80 (0.79-4.13)	
Lymph node metastasis				
Negative	1	.020	1	.148
Positive	2.23 (1.14-4.36)		1.68 (0.83-3.41)	
Histological grade				
G1	1			
G2	0.82 (0.39-1.72)	.599		
G3	1.51 (0.60-4.59)	.468		
Other type (muc)	2.32 (0.66-8.13)	.190		
CA19-9 (U/mL)				
<300	1	.024	1	.045
≥300	2.16 (1.11-4.21)		2.02 (1.02-4.00)	
Perioperative chemotherapy				
–	1	.097		
+	0.536 (0.26-1.12)			
SAA1 expression				
Negative	1	.023	1	.018
Positive	3.36 (1.18-9.55)		3.58 (1.24-10.33)	

TABLE 3 Univariate and multivariate Cox proportional hazards regression analysis of factors associated with overall survival after operation for pancreatic cancer

increased 78.5-fold by incubation with CAA-CM. *SAA1* gene knockdown using *SAA1* siRNA significantly inhibited migration/invasion capability, drug resistance, and EMT properties in PANC-1 cells (Figure 4). Consistently, *SAA1* mRNA expression was increased in all 5 pancreatic cancer cell lines to varying degrees when incubated with CM-CAA (Figure 3B). Moreover, multivariate analysis identified SAA1 as an independent prognostic marker for survival in PDAC patients. These observations clearly indicated that SAA1 expression, which was induced in pancreatic cancer cells by CAA, has a direct impact on progression with malignant phenotypes in patients with PDAC. SAA1 is a member of the apolipoprotein serum amyloid A (SAA) family and is an acute phase protein produced mainly by hepatocytes (Figure 5C) in response to proinflammatory cytokines such as IL-1β, IL-6, and TNFα.[37] Interestingly, Yang and associates recently reported that SAA1 was expressed in breast cancer cells and in tumor-associated macrophages, and that its expression is associated with worse relapse-free survival.[30] More recently, Djurec and colleagues reported that *SAA1* mRNA was expressed in human CAF and in pancreatic cancer cells as determined

by real-time PCR.[38] In the present study, we found that SAA1 protein was expressed in pancreatic cancer cells of PDAC tissues and that SAA1 was also weakly expressed in CAF surrounding the cancer cells (Figure S8). Expression levels of *SAA1* mRNA and SAA1 protein in CAF should be further investigated in future large-scale studies. Regardless, as SAA1 is a secreted protein, it appears that SAA1 plays a pivotal role in the microenvironment of PDAC tissue to promote progression of pancreatic cancers, leading to a poor prognosis.

We did not investigate the detailed mechanism by which SAA1 promoted migration/invasion capability, drug resistance, and EMT phenotypes in pancreatic cancer. However, it has been reported that SAA1 activates the transcriptional factor nuclear factor kappa B (NF-κB).[39,40] NF-κB has been reported to be involved in cell invasion and migration, drug resistance, and EMT phenotype.[39-42] In this context, we knocked down the *SAA1* gene in PANC-1 and PK-1 cells and found that migration/invasion, drug resistance, and EMT phenotype were enhanced in those cells presumably via NF-κB activation. This finding is also supported by our data showing that *SAA1*

knowdown in PANC-1/PK-1 cells led to decreased expression levels of phospho-p65, a protein downstream of NF-κB, and conversely, that phospho-p65 levels in PANC-1/PK-1 cells were increased by incubation with CAA-CM (Figure S9).

The multivariate analysis for OS in PDAC patients revealed that SAA1 expression and high CA19-9 were independent prognostic markers for OS. This result for SAA1 is explained by the in vitro data showing that SAA1 enhanced cell invasion/migration capability, drug resistance, and EMT phenotype. The results identifying CA19-9 as a prognostic marker are consistent with findings in a previous report.[43]

One of the limitations of this study is that we assessed SAA1 expression only in resectable PDAC tissues, which accounted for less than one-fifth of diagnosed PDAC cases. Therefore, further studies are necessary to confirm these findings in more advanced unresectable metastatic PDAC.

In conclusion, we demonstrated that pancreatic cancer cells induce significant change in adipocytes, leading to their de-differentiation and fibrotic changes to CAA. We also found that CAA markedly upregulated SAA1 expression, which enhanced migration/invasion capability, drug resistance, and EMT properties in pancreatic cancers. SAA1 could be a potential biomarker for a poor prognosis after surgery, and also the basis for a novel therapeutic strategy, targeting interactions between pancreatic cancer cells and peripancreatic adipose.

DISCLOSURE

The authors have no conflict of interest.

ORCID

Masanori Takehara https://orcid.org/0000-0002-9024-4900
Tetsuji Takayama https://orcid.org/0000-0002-0175-1573

REFERENCES

1. Apte MV, Xu Z, Pothula S, et al. Pancreatic cancer: the microenvironment needs attention too!. *Pancreatology.* 2015;15:S32-S38.
2. Vincent A, Herman J, Schulick R, et al. Pancreatic cancer. *Lancet.* 2011;378(9791):607-620.
3. Hall BR, Cannon A, Atri P, et al. Advanced pancreatic cancer: a meta-analysis of clinical trials over thirty years. *Oncotarget.* 2018;9(27):19396-19405.
4. Müerköster S, Wegehenkel K, Arlt A, et al. Tumor stroma interactions induce chemoresistance in pancreatic ductal carcinoma cells involving increased secretion and paracrine effects of nitric oxide and interleukin-1beta. *Cancer Res.* 2004;64(4):1331-1337.
5. Erkan M, Michalski CW, Rieder S, et al. The activated stroma index is a novel and independent prognostic marker in pancreatic ductal adenocarcinoma. *Clin Gastroenterol Hepatol.* 2008;6(10):1155-1161.
6. Xie D, Xie K. Pancreatic cancer stromal biology and therapy. *Genes Dis.* 2015;2(2):133-143.

7. Nielsen MFB, Mortensen MB, Detlefsen S. Key players in pancreatic cancer-stroma interaction: Cancer-associated fibroblasts, endothelial and inflammatory cells. *World J Gastroenterol.* 2016;22(9):2678-2700.
8. Peng C, Liu J, Yang G, et al. The tumor-stromal ratio as a strong prognosticator for advanced gastric cancer patients: proposal of a new TSNM staging system. *J Gastroenterol.* 2018;53(5):606-617.
9. Hwang RF, Moore T, Arumugam T, et al. Cancer-associated stromal fibroblasts promote pancreatic tumor progression. *Cancer Res.* 2008;68(3):918-926.
10. Gok Yavuz B, Gunaydin G, Gedik ME, et al. Cancer associated fibroblasts sculpt tumour microenvironment by recruiting monocytes and inducing immunosuppressive PD-1 + TAMs. *Sci Rep.* 2019;9(1):1-15.
11. Lonardo E, Frias-Aldeguer J, Hermann PC, et al. Pancreatic stellate cells form a niche for cancer stem cells and promote their self-renewal and invasiveness. *Cell Cycle.* 2012;11(7):1282-1290.
12. Leal AS, Misek SA, Lisabeth EM, et al. The Rho/MRTF pathway inhibitor CCG-222740 reduces stellate cell activation and modulates immune cell populations in Kras G12D; Pdx1-Cre (KC) mice. *Sci Rep.* 2019;9(1):1-12.
13. Ikenaga N, Ohuchida K, Mizumoto K, et al. CD10+ pancreatic stellate cells enhance the progression of pancreatic cancer. *Gastroenterology.* 2010;139(3):1041-1051, 1051.e1-8.
14. Theunissen J-W, de Sauvage FJ. Paracrine Hedgehog Signaling in Cancer. *Cancer Res.* 2009;69(15):6007-6010.
15. Engels B, Rowley DA, Schreiber H. Targeting stroma to treat cancers. *Semin Cancer Biol.* 2012;22(1):41-49.
16. Neesse A, Algül H, Tuveson DA, et al. Stromal biology and therapy in pancreatic cancer: a changing paradigm. *Gut.* 2015;64(9):1476-1484.
17. Olive KP, Jacobetz MA, Davidson CJ, et al. Inhibition of Hedgehog signaling enhances delivery of chemotherapy in a mouse model of pancreatic cancer. *Science.* 2009;324(5933):1457-1461.
18. Aune D, Greenwood DC, Chan DSM, et al. Body mass index, abdominal fatness and pancreatic cancer risk: a systematic review and non-linear dose-response meta-analysis of prospective studies. *Ann Oncol Off J Eur Soc Med Oncol.* 2012;23(4):843-852.
19. Cascetta P, Cavaliere A, Piro G, et al. Pancreatic cancer and obesity: molecular mechanisms of cell transformation and chemoresistance. *Int J Mol Sci.* 2018;19(11):3331.
20. Murphy N, Jenab M, Gunter MJ. Adiposity and gastrointestinal cancers: epidemiology, mechanisms and future directions. *Nat Rev Gastroenterol Hepatol.* 2018;15(11):659-670.
21. Jamieson NB, Foulis AK, Oien KA, et al. Peripancreatic fat invasion is an independent predictor of poor outcome following pancreaticoduodenectomy for pancreatic ductal adenocarcinoma. *J Gastrointest Surg.* 2011;15(3):512-524.
22. Grippo PJ, Fitchev PS, Bentrem DJ, et al. Concurrent PEDF deficiency and Kras mutation induce invasive pancreatic cancer and adipose-rich stroma in mice. *Gut.* 2012;61(10):1454-1464.
23. Philip B, Roland CL, Daniluk J, et al. A high-fat diet activates oncogenic Kras and COX2 to induce development of pancreatic ductal adenocarcinoma in mice. *Gastroenterology.* 2013;145(6):1449-1458.
24. Dawson DW, Hertzer K, Moro A, et al. High-fat, high-calorie diet promotes early pancreatic neoplasia in the conditional KrasG12D Mouse Model. *Cancer Prev Res.* 2013;6(10):1064-1073.
25. Bochet L, Lehuédé C, Dauvillier SS, et al. Adipocyte-derived fibroblasts promote tumor progression and contribute to the desmoplastic reaction in breast cancer. *Cancer Res.* 2013;73(18):5657-5668.
26. Eatrice Dirat B, Bochet L, Dabek M, et al. Cancer-associated adipocytes exhibit an activated phenotype and contribute to breast cancer invasion. *Cancer Res.* 2011;71(7):2455-2465.
27. Kang SU, Kim HJ, Kim DH, et al. Nonthermal plasma treated solution inhibits adipocyte differentiation and lipogenesis in 3T3-L1 preadipocytes via ER stress signal suppression. *Sci Rep.* 2018;8(1):1-12.

28. Tomonari T, Takeishi S, Taniguchi T, et al. MRP3 as a novel resistance factor for sorafenib in hepatocellular carcinoma. *Oncotarget.* 2016;7(6):7207-7215.

29. Muguruma N, Okamoto K, Nakagawa T, et al. Molecular imaging of aberrant crypt foci in the human colon targeting glutathione S-transferase P1–1. *Sci Rep.* 2017;7(1):6536.

30. Yang M, Liu F, Higuchi K, et al. Serum amyloid A expression in the breast cancer tissue is associated with poor prognosis. *Oncotarget.* 2014;7(24):35843-35852.

31. Lamouille S, Xu J, Derynck R. Molecular mechanisms of epithelial-mesenchymal transition. *Natl Rev Mol Cell Biol.* 2014;15(3):178-196.

32. Zoico E, Darra E, Rizzatti V, et al. Adipocytes WNT5a mediated dedifferentiation: a possible target in pancreatic cancer microenvironment. *Oncotarget.* 2016;7(15):20223-20235.

33. Wu Q, Li B, Li Z, et al. Cancer-associated adipocytes: key players in breast cancer progression. *J Hematol Oncol.* 2019;12:1-15.

34. Cui R, Yue W, Lattime EC, et al. Targeting tumor-associated macrophages to combat pancreatic cancer. *Oncotarget.* 2016;7(31):50735-50754.

35. Feygenzon V, Loewenstein S, Lubezky N, et al. Unique cellular interactions between pancreatic cancer cells and the omentum. *PLoS One.* 2017;12(6):e0179862.

36. Au Yeung CL, Co NN, Tsuruga T, et al. Exosomal transfer of stroma-derived miR21 confers paclitaxel resistance in ovarian cancer cells through targeting APAF1. *Nat Commun.* 2016;7(1):11150.

37. Jensen LE, Whitehead AS Regulation of serum amyloid A protein expression during the acute-phase response. *Biochem J.* 1998;334(3):489-503.

38. Djurec M, Graña O, Lee A, et al. Saa3 is a key mediator of the protumorigenic properties of cancer-associated fibroblasts in pancreatic tumors. *Proc Natl Acad Sci.* 2018;115(6):201717802.

39. Siegmund SV, Schlosser M, Schildberg FA, et al. Serum amyloid a induces inflammation, proliferation and cell death in activated hepatic stellate cells. *PLoS One.* 2016;11(3):1-17.

40. Lee HY, Kim MK, Park KS, et al. Serum amyloid A stimulates matrix-metalloproteinase-9 upregulation via formyl peptide receptor like-1-mediated signaling in human monocytic cells. *Biochem Biophys Res Commun.* 2005;330(3):989-998.

41. Folgueras AR, Pendas AM, Sanchez LM, et al. Matrix metalloproteinases in cancer: from new functions to improved inhibition strategies. *Int J Dev Biol.* 2004;48(5-6):411-424.

42. Zheng X, Carstens JL, Kim J, et al. Epithelial-to-mesenchymal transition is dispensable for metastasis but induces chemoresistance in pancreatic cancer. *Nature.* 2015;527(7579):525-530.

43. Dell'Aquila E, Fulgenzi CAM, Minelli A, et al. Prognostic and predictive factors in pancreatic cancer. *Oncotarget.* 2020;11(10):924-941.

SUPPORTING INFORMATION

Additional supporting information may be found online in the Supporting Information section.